

Microstructural characterisation of organic-rich shale before and after pyrolysis



Lead author
Yulia
Uvarova

Y. Uvarova¹, A. Yurikov^{1,2}, M. Pervukhina¹, M. Lebedev³,
V. Shulakova¹, M.B. Clennell¹ and D.N. Dewhurst¹

¹CSIRO Earth Science and Resource Engineering
Australian Resources Research Centre (ARRC)
26 Dick Perry Avenue
Kensington, WA 6151

²Moscow Institute of Physics and Technology
9 Institutskiy per,
Dolgoprudny, Moscow Region 141700
Russian Federation

³Department of Exploration Geophysics
Curtin University
26 Dick Perry Avenue
Kensington, WA 6151
yulia.uvarova@csiro.au

ABSTRACT

Organic-rich shales, traditionally considered as source rocks, have recently become an ambitious goal for the oil and gas industry as important unconventional reservoirs. Understanding of the initiation and development of fractures in organic-rich shales is crucially important as fractures could drastically increase the permeability of these otherwise low-permeable rocks. Fracturing can be induced by rapid decomposition of organic matter caused by either natural heating, such as emplacement of magmatic bodies into sedimentary basins, or thermal methods used for enhanced oil recovery.

In this work the authors study fracture initiation and development caused by dry pyrolysis of Kimmeridge shale, which is characterised with a high total organic carbon content of more than 20%. X-ray diffraction (XRD) analysis exhibits high carbonate (both calcite and dolomite) and low clay (illite) content. Field emission gun scanning electron microscopy (FEG-SEM) shows that kerogen is presented either as a load-bearing matrix or as a filling of the primary porosity with pores being of micron size. Cylindrical samples of the Kimmeridge shale are heated up to temperatures in the range of 330–430°C. High-resolution X-ray microtomographic (micro-CT) images are obtained. The microtomographic images are processed using AVIZO (Visualization Sciences Group) to identify and statistically characterise large kerogen-filled pores and pre-existing and initiated cracks. The relationship between the total area of fractures and the temperature experienced by the sample has been obtained. Total organic carbon content is determined for samples subjected to heating experiments. This approach enables a quantitative analysis of fracture initiation and development in organic-rich shales during heating.

KEYWORDS

Organic-rich shales, kerogen, dry pyrolysis, Kimmeridge shale, fractures, heating, micro-CT scanning, microstructures, total organic carbon.

INTRODUCTION

Recently, increased interest in unconventional resources has resulted in a large number of theoretical and experimental studies of organic-rich shales (e.g. Patrusheva et al, 2014; Far et al, 2013; Sayers, 2013; Yan and Han, 2013; Lucier et al, 2011; Loseth et al, 2011; Vanorio et al, 2008; Peters et al, 2004; Carsione, 2001). Suarez-Rivera and Fjaer (2013) studied the coupled effects of rock deformation and pore pressure on two organic-rich shales, and reported poroelastic constants of 0.3–0.6 and 0.1–0.8 for the Haynesville and Bossier shales, respectively. Such low values indicate that these shales are stiff and have low porosity. Carcione et al (2011) theoretically studied the effects of kerogen fraction and partial saturation on elastic properties of organic-rich shales at different frequencies. Sayers (2013) used the database provided by Vernik and Liu (1997) to test three different effective medium theories. The effective field theory by Sevostianov et al (2005) strongly supports the experimental results, which show that clay and kerogen form interconnected matrices in which both constituents are load-bearing.

Changes in petrophysical properties caused by heating are practically important for the production of oil and gas from low permeable shales. Zargari et al (2013) investigated elastic properties of Bakken shale with various maturation levels on samples from different depths. The samples were then subjected to hydrous pyrolysis to mimic process of natural maturation, and microstructures and local mechanical properties were compared with the same observations on the intact samples. The authors implied that an increase in Young's modulus with maturity in naturally matured shales is related to the reduction in their TOC content. Interestingly, the samples showed lower Young's moduli after the hydrous pyrolysis. The authors explained this seeming discrepancy with the fact (confirmed with SEM observations) that part of the bitumen produced during pyrolysis was trapped in the kerogen. This bitumen lowered average elastic moduli as Young's modulus of bitumen (below 2 GPa) is lower than that of kerogen.

Fracturing is considered to be a way to increase permeability of unconventional reservoirs (e.g. Lash and Engelder, 2005). Hydraulic fracturing is the most successful if the newly developed fractures connect preexisting fracture networks caused for instance by maturation processes (e.g. Far et al, 2013; Lucier et al, 2011). Pyrolysis of the kerogen in organic-rich shales partially mimics the maturation process and this can be used to study fracture network nucleation, development and propagation (e.g. Kobchenko et al, 2011; Zargari et al, 2013; Panahi et al, 2013). Kobchenko et al (2011) studied pore microstructure of the Green River Shale before and after pyrolysis, and Tiwari et al (2013) characterised pore microstructure and estimated flow properties of the Green River oil shale after pyrolysis. Theoretical and numerical modelling of cracks propagation and coalescence were provided in a number of studies (e.g. Ozkaya, 1988; Jin et al, 2010).

The authors examined fracturing in the Kimmeridge organic-rich shale during heating. Results of pyrolysis of the

shale samples heated up to several temperatures in a range of 330°C–430°C. The authors investigated the pore structure before and after heating by using high resolution microtomography. This paper also presents a full characterisation of the Kimmeridge shale before pyrolysis, including its mineralogy, distribution of the organic matter and original porosity.

ANALYTICAL TECHNIQUES AND EXPERIMENTAL PROCEDURES

Kimmeridge shale from the Upper Jurassic Kimmeridge Clay Formation is selected for this study. The Upper Jurassic Kimmeridge Clay Formation is a suite of sediments comprised of clays, carbonates, bituminous shales and oil shales (William and Douglas, 1984). The Kimmeridge Clay Formation contains shales with some of the highest total organic carbon (TOC) contents (Curtis et al, 2012a). As rock mineralogy is crucial in shale evaluation and affects its brittleness (Bai et al, 2013), the sample studied is fully characterised by powder X-Ray Diffraction (XRD), portable X-Ray Fluorescence Spectrometry (pXRF), Field-Emission Gun Scanning Electron Microscopy (FEG-SEM) at ARRC laboratories (CSIRO, Kensington WA), and computed tomography scanner (Micro-CT) at the National Geosequestration Laboratory. The TOC content is determined as well.

The shale sample is crushed, mixed with ethanol and placed on a glass slide. Powder XRD data for the sample is obtained using a Bruker D4 Endeavor AXS instrument operating with Co radiation. The X-ray diffractogram is collected for the range of 2 θ from 5°C to 90°C, with increment of 0.02°C and scan speed of 0.1. The obtained X-ray diffractogram pattern is interpreted using the DIFFRAC.EVA Bruker software package. The minerals present in the sample were identified and their percentages were estimated.

A hand sample of the shale was then analysed with a Delta hand-held pXRF spectrometer, with a large area SDD detector, integrated vacuum technology and customised 4W X-Ray tube, providing increased light-element sensitivity. The data are collected in Geochem Ba mode, which gave a range of elements analysed from Mg to U. Prior to the measurement of element concentrations by pXRF, the instrument is calibrated using a metal disk. An instrument check is done prior to and after measurements using standards: NIST 2702, NIST 2781, NIST 2710a, NIST 2711a and a SiO₂ blank (pure quartz). Detection limits are estimated on the basis of reproducibility on the measurements for certified reference materials (NIST standards). The data are reported in element wt.% or ppm for elements where concentration was above the detection limit.

A polished slab of the shale is chromium-coated and is studied using a Zeiss Ultra-Plus FEG-SEM coupled with a Bruker X-Flash EDX detector for elemental analysis. An accelerating voltage of 20 kV and a beam current of 3 nA was used. Back-scattered electron images are taken and element maps are collected to document the distribution of chemical elements, carbon in particular.

Total organic content of the shale sample is measured by the National Measurement Institute. A number of measurements are done namely on an intact sample and on samples heated to various temperatures from 330°C to 430°C.

As for studying fractures nucleation and propagation processes in shales during heating, two cylindrical samples of 5 mm height and 2 mm in diameter are prepared. The experimental procedure for each sample is described in details below:

1. To visualise pre-existing fractures, the first sample is scanned with an XRadia VersaXRM-500 micro-CT scanner with a resolution (pixel size) of 3.5 micron.
2. The sample is then heated in an OmegaLux LMF-3550 furnace (Omega, Ltd.) from room temperature to 430°C at the rate of 8°C per minute. At the final stage of heating, the

sample is maintained under the temperature of 430°C for 10 minutes. Then after cooling to room temperature another microtomographic image is obtained with the same micro-CT scanner.

3. The second sample is heated up from the room temperature to 330°C at the rate of 8°C per minute and then kept at the maximum temperature for 10 minutes. The sample is then cooled down and a microtomographic image of the sample is obtained with the same micro-CT scanner.
4. The step 3 is repeated for the temperatures of 370°C and 390°C.

For better understanding of physical and chemical processes in shales during heating, the mass loss and the TOC content during heating was measured. As the samples used for the micro-CT imaging are too small for reliable measurements of the mass loss and the TOC content, another set of four samples of the same shale is prepared and heated up to 330°C, 370°C, 390°C and 430°C. The weight and the TOC content of each sample is measured before and after heating.

To characterise the pre-existing fractures and the fractures introduced as a result of heating the samples, obtained microtomograms are processed using AVIZO software (Visualisation Sciences Group). The data initially come as a series of greyscale 2D images saved in a tagged image file format. Each greyscale 2D image is a set of numbers corresponding to X-ray densities assigned to each voxel of the scanned volume. These micro-CT images cannot be directly used for the analysis; they require pre-processing and segmentation into a mineral matrix phase and a void/fracture phase. The processing routine started from stacking the series of 2D images together to form 3D volumes of 700 × 700 × 1,000 voxels. Then all five volumes were cropped to the smaller cubes of 400 × 400 × 400 voxels from the center of the original microtomogram. This was done to avoid the effect of beam hardening on the intensity of the microtomogram, as well as the edge effects that could influence fractures characteristics on the edge of the sample as a result of inhomogeneous heating.

To enhance the signal-to-noise ratio of the micro-CT images, a 3D Gaussian filter and a 3D median smoothing filter were applied. As a result, most of the random speckle noises are removed from the tomogram, whereas the important features of the original image, such as fractures are preserved. At the next step, the grey-scale 3D volumes are transformed to binary ones, where each voxel represented mineral matrix or void space (pore or fracture). The routine is based on a simple threshold (histogram-based) algorithm, which assigned labels to voxels according to their intensities. The threshold levels are chosen interactively for each of five volumes. The noise remained after the data enhancement algorithms results in the presence of small isolated objects on the labelled volumes. These objects may degrade the data quality and affect further statistical analysis. Thus, all the objects below the volume threshold of 15 voxels are excluded from the process. The detailed description of the image processing procedure can be found in Shulakova et al (2012).

COMPOSITION AND 2D MICROSTRUCTURE

A composition and 2D microstructure of a sample from the Kimmeridge shale before heating is fully characterised using XRD, pXRF and FEG-SEM techniques. According to Curtis et al (2012a), shales of Kimmeridge Clay Formation have the highest TOC values reported in the literature. The sample studied here has the TOC content of 23.4% (Table 1), which is in the range of previously reported values of 6–49 wt.% (Curtis et al, 2012a). The TOC content is also measured for the shale samples heated up to a range of temperatures and it decreases with increasing temperature of pyrolysis (Table 1).

The XRD study of the Kimmeridge shale shows that the rock is characterised by high carbonate content, which constituted around 40 % (total percentage of calcite and dolomite) and low illite content (~ 6%) (Table 2). Framework silicates include feldspars and quartz at 28%, and pyrite constitutes 1% of the total rock volume (Table 2). The presence of some crystalline organic compound is identified. The peaks on the powder XRD pattern match a compound with the chemical formula of $C_{14}H_{18}O_7$ (Fig. 1). This is an interesting observation because crystalline organic matter is not common while amorphous organic matter is the predominant type of organic matter in shales with low thermal maturity (Curtis et al, 2012b).

The chemical composition of Kimmeridge shale is quite simple with: Si, Ca, Mg, Al, Fe and K being the major elements and having concentrations at percent level (Table 3). Light elements, namely carbon and oxygen, are not determined by portable XRF but are main constituents and comprise approximately 52% (Table 3).

Minerals in the Kimmeridge shale contain elements with atomic numbers higher than carbon, and it is therefore possible to distinguish organic matter from inorganic minerals by the darker colour of kerogen in back-scattered electron (BSE) images. The sample was characterised with the FEG-SEM which allows element mapping, documentation of rare micron-scale features in geologic samples and the distribution of trace elements in heterogeneous samples. The element mapping done on the sample of Kimmeridge shale shows the distribution of kerogen in the sample (Figures 2 and 3). The carbon-containing inorganic carbonates (calcite and dolomite) are green on the composite-coloured map in Figure 2, as they contain Ca and Mg, and kerogen is red. The organic component of the sample acts as a groundmass and encapsulates grains of minerals (Figures 2 and 3).

The Kimmeridge shale exhibits two primary porosity textures: organic and inorganic. There are fractures and voids or pores in the kerogen part of the sample (Figures 2, 4, 5, 6 and 7). Some primary fractures are up to 10 μm long and 0.5 μm wide (Fig. 2). Voids or pores in the studied sample are of the sub-micron size (Fig. 4) and are commonly located in the kerogen groundmass in close proximity or on the boundary with mineral grains (Figures 5 and 6). From the FEG-SEM images, the authors estimate the organic porosity to be on the order of 6–10%. Significant inorganic porosity is associated with carbonates. Mineral grains often have crack-like fractures (Fig. 2) and pores or voids in them of up to a few microns in size (Fig. 7).

3D MICROSTRUCTURE BEFORE AND AFTER HEATING

Slices from each of the five microtomograms obtained for the original sample of the Kimmeridge shale at 25°C and then heated to 330°C, 370°C and 390°C, and the sample heated up to the temperature of 430°C are shown in Figure 8. These images are obtained perpendicular to bedding plane and illustrate fracture nucleation and development as a result of the heating process. The weight loss and the TOC content of each of the samples before and after heating is shown in Table 4.

The intact shale (Fig. 8a) exhibits a typical layered structure with few fractures of the 2–5 pixel (7–18 micron) width. Due to insufficient resolution, it is difficult to distinguish between the non-organic shale constituents and kerogen, which might be distinguishable as darker spots due to its lower density in more detailed images. The growth and development of fractures resulting from the increase in experienced temperature is clearly visible (Figures 8b and c). The developed fracture network is highly anisotropic as the fracture growth occurs parallel to the bedding plane with just a few cracks developed at an acute angle with the bedding. In the temperature range of 370°C–390°C the significant increase of fracture length is observed

Table 1. Total organic carbon (TOC) content of the shale samples at room temperature and heated in the range from 25°C–430°C.

Measurement	TOC %	Experimental conditions
Sample 1	23.4	Room temperature
Sample 2	22.9	Heated up to 330°C
Sample 3	19.7	370°C
Sample 4	7.9	390°C
Sample 5	0.8	430°C
Sample 6	1.3	Heated up to 390°C twice

Table 2. Semi-quantitative mineral percentages determined by powder XRD and TOC content analysis.

Mineral	Mineral formula	Mineral %
Quartz	SiO_2	9.2
Pyrite	FeS_2	0.8
Oligoclase	$\text{Na}_{0.8}\text{Ca}_{0.2}\text{Al}_{1.2}\text{Si}_{2.8}\text{O}_8$	15.7
Microcline	KAlSi_3O_8	3.2
Illite	$\text{KAl}_2[\text{AlSi}_3\text{O}_{10}](\text{OH})_2$	5.6
Calcite	CaCO_3	20.8
Dolomite	$\text{CaMg}(\text{CO}_3)_2$	21.3
Total organic carbon		23.4

(Figures 8c–d). This indicates that at this temperature range, the rapid growth and coalescence of fractures occur. The image of the sample presented in Figure 8e shows a little difference with the image in Figure 8d, however a lot of small black spots can be observed in the latter. This might imply that at temperatures higher than 390°C, the growth of large fractures slow down and new smaller fractures start to nucleate.

For statistical analysis of the number of isolated fractures, surface areas, shapes and all separate fractures were picked out within AVIZO by the method described in the section on analytical techniques and experimental procedures. Fracture volume, minimum and maximum size, surface area and orientation was determined for each sample. The total number of fractures in the samples that experienced different maximal temperatures is shown in Table 5. The number of the fractures stays nearly constant when the temperature increases from 25 to 330°C. With further temperature increase from 330°C–370 °C and then to 390°C, the number of fractures normalised to the number of fractures at room temperature drops drastically from 1–0.67 and to 0.43, respectively. A further temperature increase up to 430°C leads to a slight increase in a number of fractures due to the nucleation of new fractures. The surface areas of fractures was also analysed for each of the samples. The results are shown in Figure 9. It can be seen that with the increase of the temperature the size of the cracks increases. For example, while at room temperature, the size of the surface area of the largest fractures is ~ 40 thousand square pixels, the same size is about 7 times larger at 330°C and its 15 times larger at 430°C. The number of cracks with a particular surface area decreases overall with increase of the surface area. The number of large fractures (with the surface area above ~40 thousand square pixels) increases with the increase of the experienced temperature. The number of small fractures (with the area of less than ~ 8 thousand square pixels) first decreases up to the

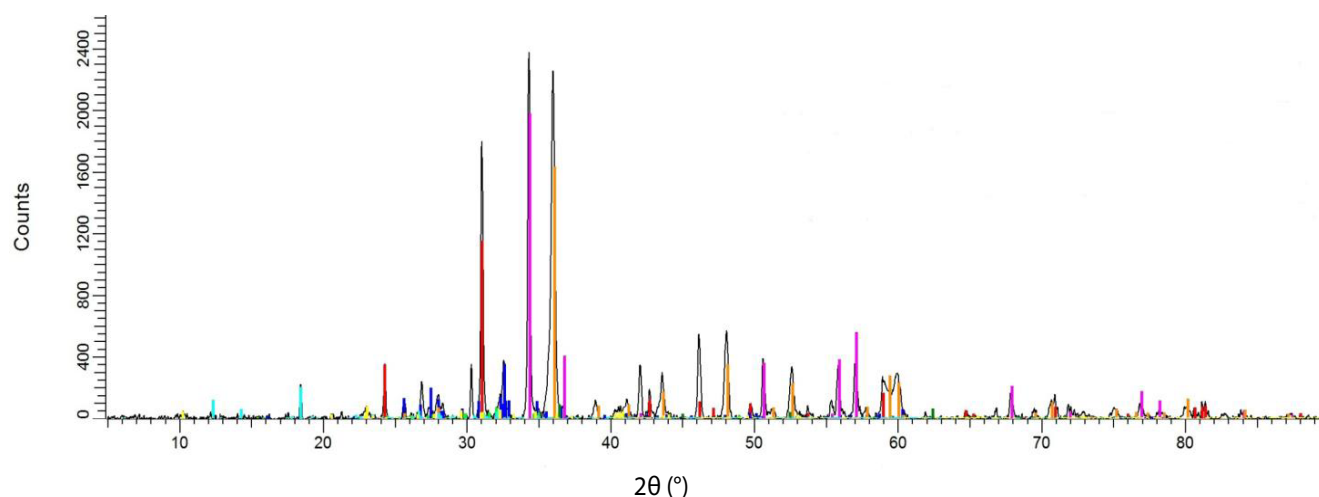


Figure 1. The Powder X-Ray Diffraction (powder XRD) pattern of the Kimmeridge shale. Minerals and compounds identified in the sample are presented by the following colours: quartz—red; oligoclase—dark blue; microcline—bright green; calcite—pink; dolomite—orange; illite—yellow; pyrite—green; and, crystalline organic phase—blue.

Table 3. Chemical composition of the Kimmeridge shale.

Element	Unit	Concentration
Al	%	4.83
As	ppm	35
Bi	ppm	8
Ca	%	13.47
Co	ppm	8
Cu	ppm	38
Fe	%	1.46
K	%	0.96
Mg	%	4.04
Mn	ppm	411
Mo	ppm	17
Pb	ppm	18
Rb	ppm	49
S	ppm	6,300
Se	ppm	4
Si	%	21.84
Sr	ppm	759
Ti	ppm	984
Y	ppm	4
Zn	ppm	49
Zr	ppm	30
LE*	%	52.77

Note: Light elements (LE) (elements with $Z < 12$ are not determined by portable X-Ray Fluorescence Spectrometry (pXRF).

temperature of 390°C and then increases again in the sample that is heated up to 430°C.

This fracture size distribution can be explained by the fact that at temperatures of 330°C–390°C, the intensive growth and coalescence of existing fractures takes place and, therefore, the overall number of fractures decreases (Table 5). This growth also explains the decrease of the number of small fractures and the increase in the number of larger fractures. While the nucleation of new small fractures take place slower than the growth of the existing ones at the temperatures of 330°C–390°C, at the

higher temperatures of 390°C–430°C, the rapid nucleation of small fractures is initiated again, along with the growth of the number of the existing cracks and the increase of the number of the large cracks. The aspect ratio of fractures in the samples that experienced different temperatures is presented in Figure 10. The histogram shows that most of the fractures have aspect ratios of 0.1–0.25 for all of the samples. The median aspect ratio is slightly higher for the samples that are heated up to 370°C, 390°C and 430°C. The occurrence frequency is higher for the intact sample and the sample that is heated to 330°C, as the total number of the isolated cracks is larger in these samples. Approximately, the same median aspect ratio of the fractures in the intact sample and ones after heating can be explained by the abundant small cracks with an aspect ratio probably distorted by the scanner resolution.

DISCUSSION

The Kimmeridge shale is characterised by one of the highest inorganic carbonate and total organic carbon content. High carbonate and low illite content suggests that the shale is brittle and prone to natural fractures. There are some crystalline organic components which might indicate that the shale is at least partially mature, as it was shown that amorphous organic matter is the predominant type in shales with low thermal maturity (Pacton et al, 2011). The organic porosity in the Kimmeridge shale was estimated to be 6–10%, which may support the hypothesis that the shale is partially thermally mature (Curtis et al, 2012b). The organic component of the sample acts as a ground-mass and encapsulates grains of minerals, indicating that the organic matter may have been mobile and encapsulated these grains (Curtis et al, 2012b).

The intensive growth and coalescence of existing fractures takes place at temperatures from 330°C–390°C. Total area of all the fractures can be calculated as a damage parameter D , which is established as the total area of fractures per unit volume (Miller et al, 1999). The dependence between D and experienced temperature shows that the fastest fracture growth occurred at the temperature range from 370°C–380°C (Fig. 11).

Total organic carbon content and weight loss analyses show that almost all kerogen is decomposed by 430°C. Thirty percent weight loss occurs after heating up to 430°C, with the initial TOC content of ca. 23% and the rest of weight loss being associated with the loss of intergranular and structural

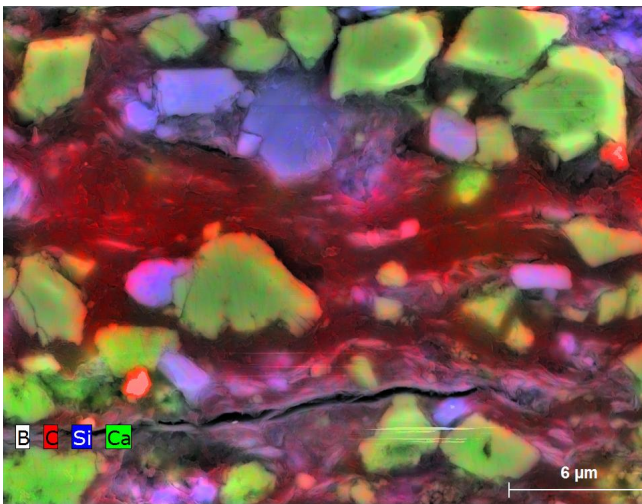


Figure 2. Element mapping using FEG-SEM for the Kimmeridge shale, showing carbon in red, silicon in blue and calcium in green. In this map, carbonates are green, silicates are blue and kerogen is red in colour. There is also a visible fracture in the kerogen matrix and a large void next to a carbonate grain.

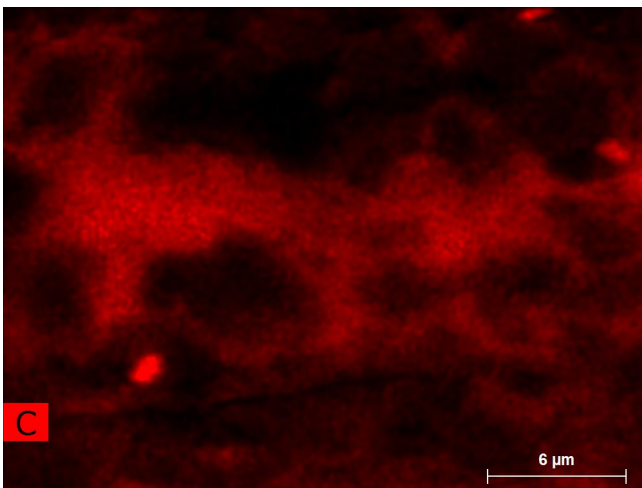


Figure 3. The carbon element map of the same area in Figure 2, showing the distribution of kerogen in the sample.



Figure 4. FEG-SEM image of the Kimmeridge shale, showing a void measuring at around 1 μm in the original sample.

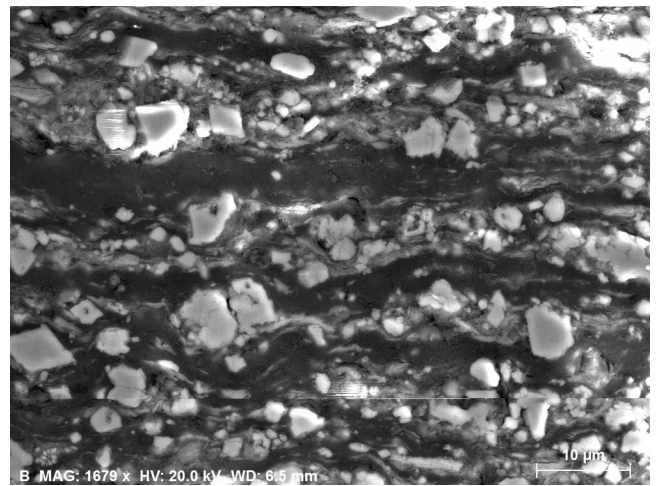


Figure 5. FEG-SEM image of the sample, showing the distribution of kerogen (dark grey colour) in the sample.

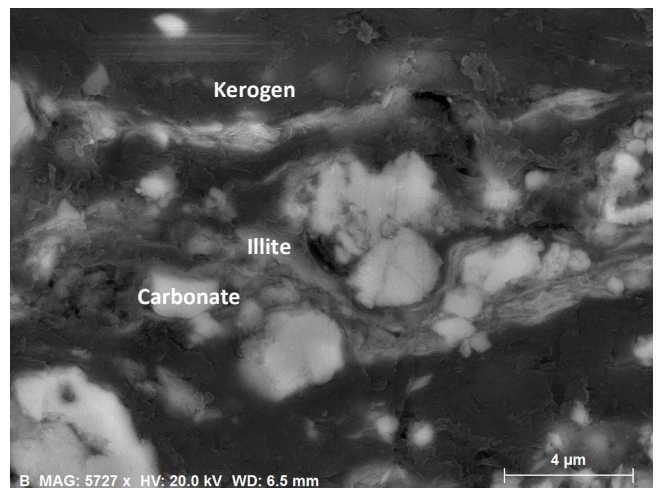


Figure 6. BSE FEG-SEM image of the Kimmeridge shale displaying primary porosity in the kerogen.

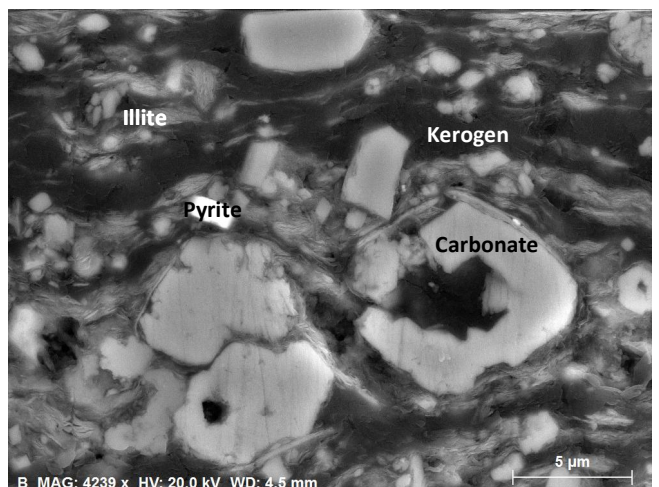


Figure 7. BSE FEG-SEM image of the Kimmeridge shale displaying inorganic porosity mostly associated with carbonates.

Continued next page.

Continued from previous page.

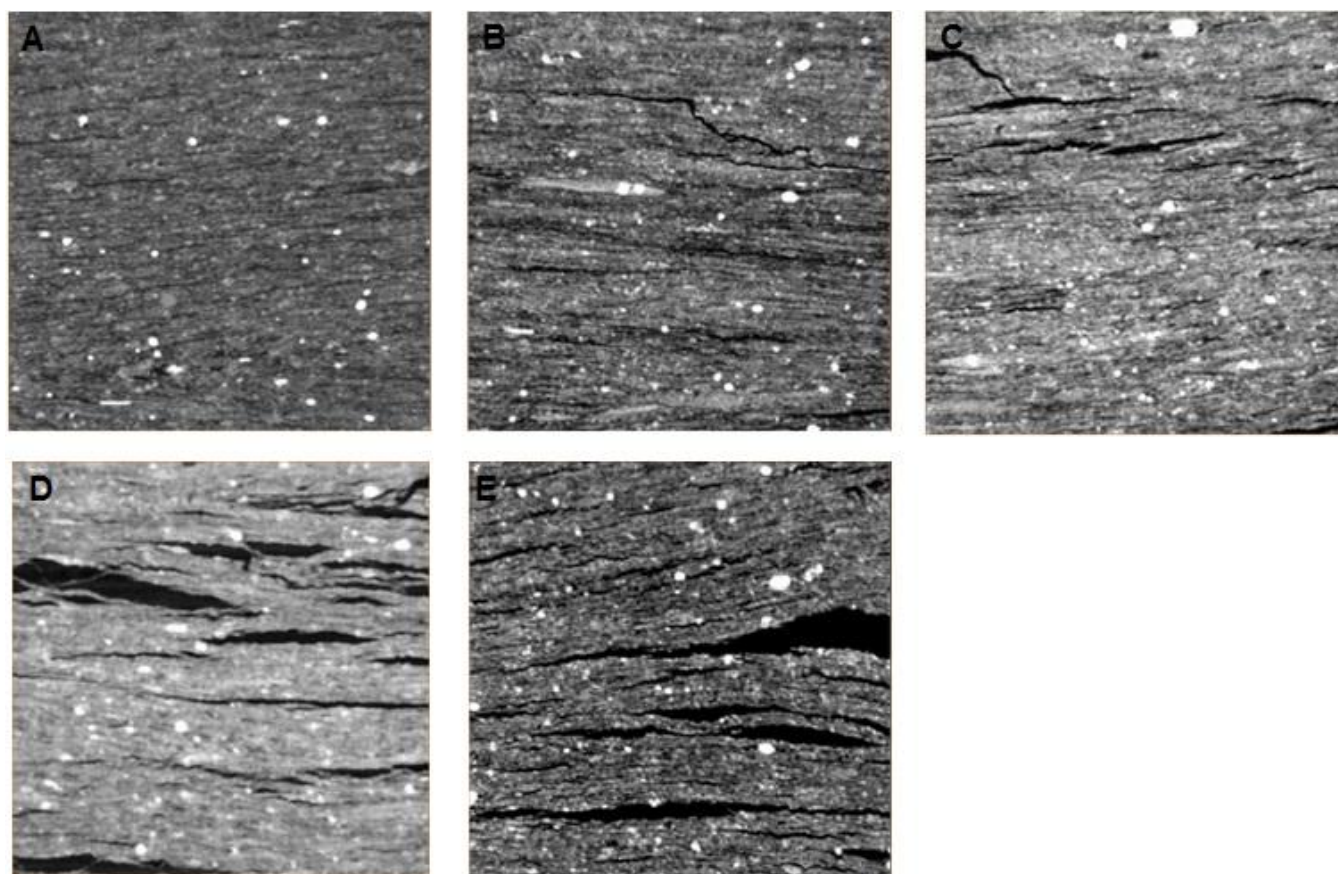


Figure 8. Micro-CT grey scale images (400×400 pixels² or 1.4×1.4 mm²) of the Kimmeridge shale: A) the sample of the untreated shale at 25°C where tiny microcracks (2-5 pixels wide) are observed; B) the sample at 330°C where nucleation of fractures begins; C) at 370°C, propagation and coalescence of several fractures are observed; D) at 390°C, fast growth of fractures is observed; and, E) at 430°C, a little difference with previous slice (D) is observed.

Table 4. Weight loss and TOC content measurements after heating.

#	Weight (g) at room T	Weight (g) after heating	Weight loss (%)	TOC (%)
1	0.79	330°C 0.75	5	22.9
2	0.96	370°C 0.89	7	19.7
3	0.85	390°C 0.65	24	7.9
4	1.18	430°C 0.83	30	0.8

Table 5. The number of isolated fractures observed in the microtomograms.

T (°C)	Absolute number of fractures	Normalised number of fractures*
25	4,525	1
330	4,227	0.93
370	3,046	0.67
390	1,947	0.43
430	2,711	0.60

* Number of fractures normalised to the initial number of fractures observed at room temperature.

Continued next page.

Continued from previous page.

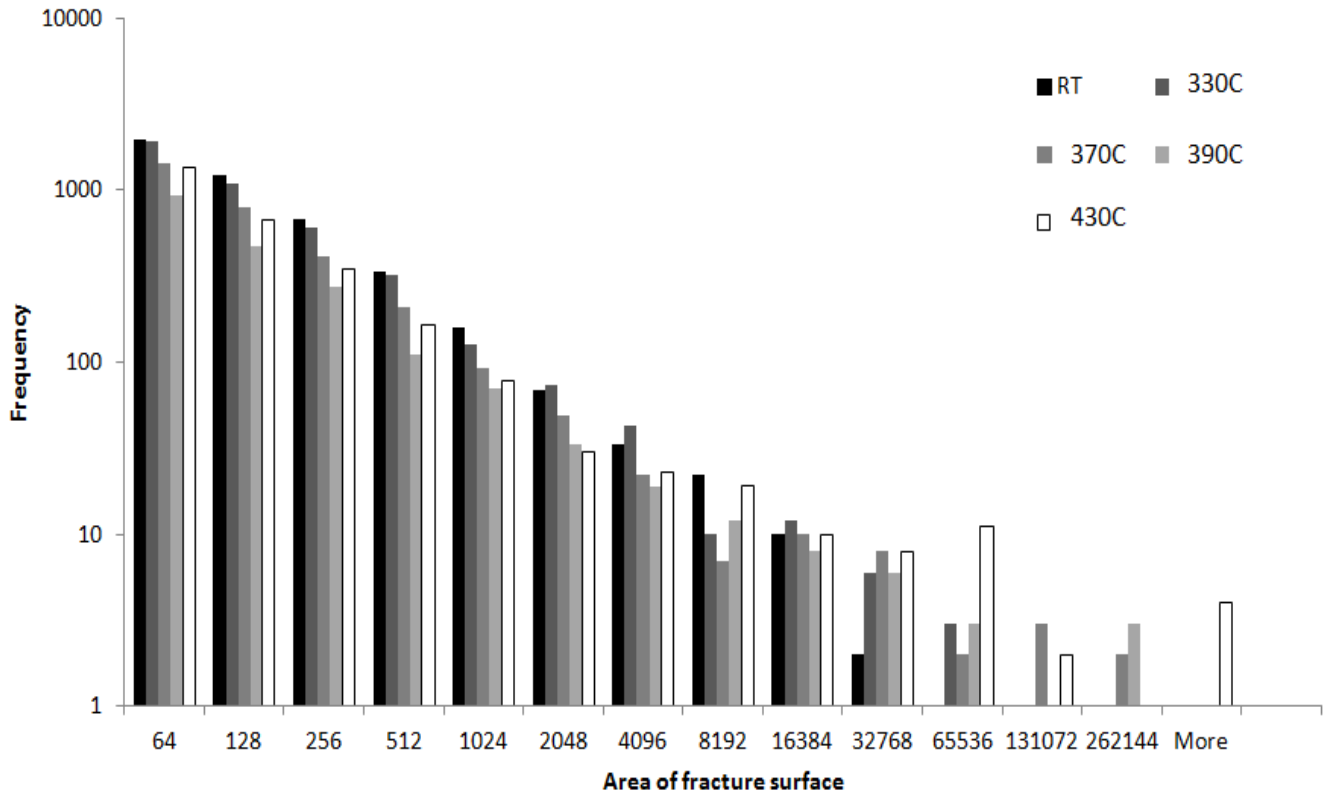


Figure 9. Histogram of fracture surface areas. The number of large fractures (with the surface area above ~ 40 thousand square pixels) increases with the increase of the experienced temperature. The number of small fractures (with the area of less than ~ 8 thousand square pixels) first decreases up to the temperature of 390°C and then increases again in the sample that is heated up to 430°C.

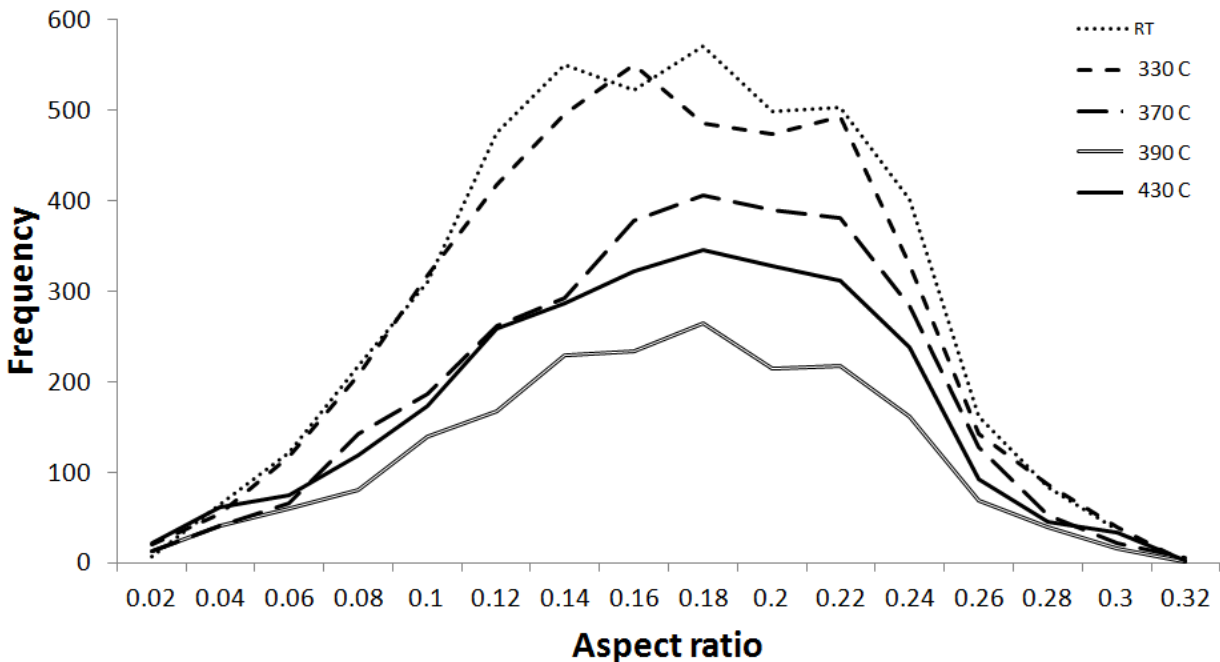


Figure 10. Histogram of aspect ratio of fractures for each experienced temperature. Most of the fractures have aspect ratios of 0.1–0.25 for all of the samples. The median aspect ratio is slightly higher for the samples that are heated up to 370°C, 390°C and 430°C. The occurrence frequency is higher for the intact sample and the sample that is heated to 330°C, as the total number of the isolated cracks is larger in these samples.

Continued next page.

Continued from previous page.

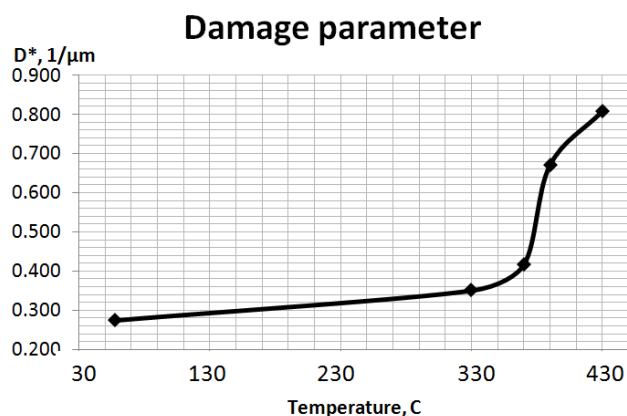


Figure 11. The relation between the damage parameter D and the temperature experienced by the shale. The dependence between D and experienced temperature shows that the fastest fracture growth occurred at the temperature range 370°C–380°C.

H₂O. The most significant amount of kerogen is decomposed at the temperature range of 370°C–390°C. This fact is supported by the decreasing growth of fracture total area after 390°C, the TOC content temperature dependence and weight loss experiment. Such results are in a good agreement with the results presented by Kobchenko et al (2011).

The obtained statistical results can be used for modelling the effects of fracture initiation, growth on elastic properties and hydraulic permeability of organic-rich shales. Further work should be done to experimentally measure the fracture-induced variations of elastic properties and permeability.

CONCLUSIONS

1. Powder XRD analysis for the Kimmeridge shale shows high carbonate content and low clay (illite) content, implying that the shale is brittle and subject to natural fractures.
2. The presence of crystalline organic matter is documented for the first time for the Kimmeridge shale.
3. The shale exhibits both organic and inorganic porosity. The pores in organic matter are either crack-like or voids and of micron size. The inorganic porosity is mostly associated with carbonates.
4. The growth and development of fractures under heating conditions starts above 300°C, with the fracture network developing parallel to the bedding plane with just a few cracks developing perpendicular to the bedding.
5. Existing fractures show significant growth at 330°C–390°C and at higher temperatures of 390°C–430°C, the rapid nucleation of small fractures is initiated along with the increasing number of the existing cracks and increasing number of the large ones.
6. The dependence between the damage parameter D and experienced temperature shows that the fastest fracture growth occurred in a narrow range of 370°C–390°C.
7. Almost all kerogen is decomposed by 430°C, as shown by the TOC content and the weight loss of the shale.
8. The obtained statistical results can be used for modelling the effects of fracture initiation, growth on elastic properties and hydraulic permeability of organic-rich shales.

ACKNOWLEDGMENTS

Alexey Yurikov was sponsored by the CSIRO Petroleum Geoscience Capability Development Fund. The work has

been supported by CSIRO Energy and Minerals Down Under National Research Flagships. Microtomograms have been obtained using the National Geosequestration Laboratory's micro-CT scanner, located at Curtin University. The authors greatly appreciate help from Michael Verrall for obtaining the FEG-SEM data.

REFERENCES

- BAI, B.J., ELGMATI, M., ZHANG, H. AND WEI, M.Z., 2013—Rock characterization of Fayetteville shale gas plays. *Fuel*, 105, 645–52.
- CARCIONE, J.M., HELLE, H.B. AND AVSETH, P., 2011—Source-rock seismic-velocity models: Gassmann versus Backus. *Geophysics*, 76 (5), N37–45.
- CARCIONE, J.M., 2001—AVO effects of a hydrocarbon source-rock layer. *Geophysics*, 66 (2), 419–27.
- CURTIS, M. SONDERGELD, C., AMBROSE, R.J. AND RAI, C.S., 2012—Microstructural investigation of gas shales in two and three dimensions using nanometer-scale resolution imaging. *The American Association of Petroleum Geologists Bulletin*, 96 (4), 665–77.
- CURTIS, M., CARDOTT, B.J., SONDERGELD, C., AND RAI, C.S., 2012b—Development of organic porosity in the Woodford Shale with increasing thermal maturity. *International Journal of Coal Geology*, 103, 26–31.
- FAR, M.E., SAYERS, C.M., THOMSEN, L., HAN, D.H. AND CASTAGNA, J.P., 2013 —Seismic characterization of naturally fractured reservoirs using amplitude versus offset and azimuth analysis. *Geophysical Prospecting*, 61 (2), 427–47.
- JIN, Z.H., JOHNSON, S.E. AND FAN, Z.Q., 2010—Subcritical propagation and coalescence of oil-filled cracks: Getting the oil out of low permeability source rocks. *Geophysical Research Letters*, 37 (L01305), 1–5.
- KOBCHENKO, M., PANAHI, H., RENARD, F., DYSTHE, D.K., MALTHE-SORENSEN, A., MAZZINI, A., SCHEIBERT, J., JAMTVEIT, B. AND MEAKIN, P., 2011—4D imaging of fracturing in organic-rich shales during heating. *Journal of Geophysical Research*, 116 (B12201), 1–28.
- LASH, G.G. AND ENGELDER, T., 2005—An analysis of horizontal microcracking during catagenesis: Example from Catskill delta complex. *The American Association of Petroleum Geologists Bulletin*, 89 (11), 1,433–49.
- LOSETH, H., WENSAAS, L., GADING, M., DUFFAUT, K. AND SPRINGER, M., 2011—Can hydrocarbon source rocks be identified on seismic data? *Geology*, 39 (12), 1,167–70.
- LUCIER, A.M., HOFMANN, R. AND BRYNDZIA, L.T., 2011—Evaluation of variable gas saturation on acoustic log data from the Haynesville Shale gas play. *Society of Exploration Geophysicists*, 30 (3), 300–11.
- MILLER, O., FREUND, L.B. AND NEEDLEMAN, A., 1999—Modeling and simulation of dynamic fragmentation in brittle materials. *International Journal of Fracture*, 96 (2), 101–25.

- OZKAYA, I., 1988—A simple analysis of oil-induced fracturing in sedimentary rocks. *Marine and Petroleum Geology*, 5 (3), 293–7.
- PACKTON, M., GORIN, G.E. AND VASCONCELOS, C., 2011—Amorphous organic matter- Experimental data on formation and the role of microbes. *Review of Paleobotany and Palynology*, 166, 253–67.
- PANAHI, H., KOBCHENKO, M., RENARD, F., MAZZINI, A., SCHEIBERT, J., DYSTHE, D., JAMTVEIT, B., MALTHE-SORENSEN, A. AND MEAKIN, P., 2013—A 4D Synchrotron X-Ray-Tomography Study of the Formation of Hydrocarbon-Migration Pathways in Heated Organic-Rich Shale. *Society of Petroleum Engineers Journal*, 18 (2), 366–77.
- PATRUSHEVA, N., LEBEDEV, M., PERVUKHINA, M., DAUTRIAT, J. AND DEWHURST, D.N., 2014—Changes in microstructure and elastic properties of Mancos shale after pyrolysis. The 76th EAGE Conference & Exhibition, Amstersdam, Netherlands, 16–19 June, Extended Abstract, submitted.
- PETERS, K.E., WALTERS, C.C. AND MOLDOWAN, J.M., 2004—The Biomarker Guide: Volume 2, Biomarkers and Isotops in Petroleum Systems and Earth History. UK:Cambridge University Press.
- SAYERS, C.M., 2013—The effect of kerogen on the elastic anisotropy of organic-rich shales. *Geophysics*, 78 (2), D65–74.
- SEVOSTIANOV, I., YILMAZ, N., KUSHCH, V. AND LEVIN, V., 2005—Effective elastic properties of matrix composites with transversely-isotropic phases. *International Journal of Solids and Structures*, 42 (2), 455–76.
- SHULAKOVA, V., PERVUKHINA, M., MÜLLER, T.M., LEBEDEV, M., MAYO, S., SCHMID, S., GOLODONIUC, P., DE PAULA, O.B., CLENELL, M.B. AND GUREVICH, B., 2012—Computational elastic up-scaling of sandstone on the basis of X-ray micro-tomographic images. *Geophysical Prospecting*, 61 (2), 287–301.
- SUAREZ-RIVERA, R. AND FJAER, E., 2013—Evaluating the poroelastic effect on anisotropic, organic-rich, mudstone systems. *Rock Mechanics and Rock Engineering*, 46 (3), 569–80.
- TIWARI, P., DEO, M., LIN, C.L. AND MILLER, J.D., 2013—Characterization of oil shale pore structure before and after pyrolysis by using X-ray micro CT. *Fuel*, 107, 547–54.
- VANORIO, T., MUKERJI, T. AND MAVKO, G., 2008—Emerging methodologies to characterise the rock physics properties of organic-rich shales. *Society of Exploration Geophysicists*, 27 (6), 780–7.
- VERNIK, L. AND LIU, X.Z., 1997—Velocity anisotropy in shales: A petrophysical study. *Geophysics*, 62 (2), 521–32.
- WILLIAM, P.F.V. AND DOUGLAS, A.G., 1984—Organic geochemistry of the British Kimmeridge Clay. 1. Composition of shale oils produced from Kimmeridge sediments. *Fuel*, 64 (8), 1,062–9.
- YAN, F.H. AND HAN, D.H., 2013—Measurement of elastic properties of kerogen. The 83rd SEG International Conference and Exhibition, Houston, Texas, 22–27 September, 2,778–82.
- ZARGARI, S., PRASAD, M., MBA, K.C. AND MATTSON, E.D., 2013—Organic maturity, elastic properties and textural characteristics of self-resourcing reservoirs. *Geophysics*, 78 (4), D223–35.

THE AUTHORS



Yulia Uvarova holds a geochemist/ exploration geochemist position in CSIRO, Minerals Down Under Flagship in Perth. Yulia works in a team of researchers developing new workflows and techniques for mapping the distal footprints of metalliferous mineral systems, through drilling and sampling and developing the science of understanding large geochemical footprints of mineral systems and their detection on the surface. Yulia graduated from the Faculty of Geology, Moscow State University with a BSc (Hons) in geology in 2001, and from the Department of Geological Sciences, University of Manitoba she got her PhD in 2008. After graduating from the University of Manitoba, Yulia undertook a research position at Queens' University, Canada, where her research focused on geochemistry, mineralogy, petrology and genesis of economic mineral deposits, uranium in particular: the development of new exploration tools for the search of U deposits; behaviour of high field strength elements (HFSE) in high-temperature systems; geochemistry of non-traditional isotopic systems; and, application of these systems to elucidate processes responsible for deposit formation.

yulia.uvarova@csiro.au



Alexey Yurikov is a candidate for a master's degree of petroleum engineering at the Moscow Institute of Physics and Technology (MIPT). His current work centers on the numerical modeling of fireflood technology in oil and gas shales. Alexey has a BSc (2012) from MIPT in applied physics and mathematics. He was an intern at CSIRO Earth Science Resource Engineering in Perth, Australia in 2013.

yurikovas@gmail.com

Continued next page.

Continued from previous page.

THE AUTHORS



Marina Pervukhina is the petrophysics team leader at CSIRO Earth Science and Resource Engineering Department. Marina is a physicist by background with a BSc and MSc in applied physics and mathematics, received from the Moscow Institute of Physics and Technology in Russia, and a PhD in geophysics from Kyoto University in Japan. Marina's main research interests are theoretical and numerical rock physics, borehole geophysics and petrophysics. Marina was designated as an outstanding reviewer for Geophysics in 2009.

marina.pervukhina@csiro.au



Valeriya Shulakova is a geophysicist by background, with expertise in digital rock physics and 4D seismics. Prior to joining CSIRO in 2008 as a research scientist, Valeriya has spent more than 7 years working for geophysical service companies in Russia. She has a BSc in Geology (2001), a MSc in Geology (2003) and a PhD (2007) all from Moscow State University in Russia.

Valeriya.Shulakova@csiro.au



David N. Dewhurst is a geologist by background with a BSc from the University of Sheffield and a PhD from the University of Newcastle, both in the UK. He has worked for over 20 years on microstructure and rock properties, with an emphasis on clay and shale behaviour. He did postdoctoral stints at the University of Birmingham, University of Newcastle, L'Institut Français du Pétrole and Imperial College before moving to CSIRO in 1998. There, he has worked on overpressure, fault and top seals and the links between geomechanics, rock physics and petrophysics in shales. David is the Research Programme Leader for Petroleum Geoscience at CSIRO, leading a team of 75 people and also is the head of the CSIRO Shale Research Centre, where he leads a consortium investigating gas shales.

david.dewhurst@csiro.au



Maxim Lebedev is an associate professor at the Department of Exploration Geophysics at the Curtin University of Technology. Maxim gained a masters of science in physics and engineering from the Moscow Institute of Physics and Technology, Russia, in 1986 and was awarded a PhD in physics from the same university in 1990. He worked for a decade as a physicist at the High Energy Research Centre in Russia, and for eight years as a material scientist at the National Institute of Advanced Industrial Science and Technology in Japan. In 2007, Maxim joined Curtin University and became the leader of an experimental group in rock physics. His research is focused on the properties of subsurface reservoir rocks and minerals. He is author and co-author of over 100 scientific papers, and has been granted six international patents.

m.lebedev@exchange.curtin.edu.au



M. Ben Clennell leads the Petroleum Exploration and Production theme in CSIRO's Energy Flagship. The theme covers onshore and offshore oil, gas research in both conventional and unconventional resources, and involves 70 full-time researchers at CSIRO research labs, located at major centres in Australia. Ben has a productive record in geological and geophysical research, and is an expert in petrophysics, natural gas hydrates in marine environments, hydrodynamics in porous media and more generally in marine and structural geology. He has led major research projects investigating both conventional and unconventional hydrocarbon reservoirs. Ben set up the petrophysics laboratories at the Australian Resource Research Centre and the X-ray CT scanning facilities, and is now helping the National Geosequestration Laboratory set up world class CO₂ core flooding facilities. As well as having a range of international networks, Ben has works in close collaboration with partners from the Western Australian Energy Research Alliance (WA-ERA) at Curtin University and the University of Western Australia, where he also supervises a number of PhD students. Ben has a bachelor degree in geology from the University of Oxford and a PhD in structural geology from the Royal Holloway University of London. He has worked as a postdoctoral researcher at the universities of Birmingham, the UK and Leeds, with links to the Ocean Drilling Program. Before moving to Australia to work at CSIRO in 2003, Ben spent five years working as a visiting professor at the Federal University of Bahia in Brazil.

ben.clennell@csiro.au